Journal of Non-Crystalline Solids 354 (2008) 3433–3437

Contents lists available at ScienceDirect

Journal of Non-Crystalline Solids

journal homepage: www.elsevier.com/locate/jnoncrysol

Silicate nanoparticles by bioleaching of glass and modification of the glass surface

Sneha Kulkarni, Asad Syed, Sanjay Singh, Anil Gaikwad, Kashinath Patil, K. Vijayamohanan, Absar Ahmad *, Satishchandra Ogale *

National Chemical Laboratory, Dr. Homi Bhabha Road, Pashan, Pune, India

ARTICLE INFO

Article history:
Received 29 September 2007
Received in revised form 12 January 2008
Available online 21 April 2008

PACS:
61.43.Fs
61.46.+w
87.68.+Z

Keywords:
Bioglass
Biomaterials
Nanoparticles
Borosilicates

ABSTRACT

Bioleaching is examined as a low temperature (50 °C) soft chemical approach to nanosynthesis and surface processing. We demonstrate that fungus based bioleaching of borosilicate glass enables synthesis of nearly monodispersed ultrafine (~5 ± 0.5 nm) silicate nanoparticles. Using various techniques such as X-ray diffraction, X-ray photoelectron spectroscopy and FTIR we compare the constitution and composition of the nanoparticles with that of the parent glass, and establish the basic similarities between the two. The bioleaching process is shown to enhance the non-bridging oxygen component and correspondingly influence the Si–O–Si network. The root mean square roughness of glass surface is seen to increase from 1.27 nm for bare glass to 2.52 nm for 15 h fungal processed case, this increase being equivalent to that for glass annealed at 500 °C.

1. Introduction

Bioleaching is a well-known process in the context of metal extraction from minerals [1–7]. However, its unique low temperature soft processing green chemistry capabilities has hardly been exploited in the context of nanosynthesis and nanoscale surface processing. Indeed, biofluids generated by micro-organisms contain multiple organic acids capable of controlled slow leaching of elements and proteins which can dynamically cap and control the growth of molecular complexes, rendering the right conditions for the synthesis of capped ultrafine nanoparticles. Most importantly this can be implemented at or near room temperature in an environmentally friendly manner.

In the case of complex compounds such as multicomponent oxides, sulphides, carbonates etc. valence-controlled synthesis of stoichiometric nanosized particles is difficult because at low temperature the proper phase may not form due to limitations of phase equilibria and at high temperature the particle size can not be easily controlled within the nano-regime. In such cases a promising approach is to start with a bulk source of the compound, either naturally extracted or synthesized by high temperature processing, and subject it to stoichiometric extraction and nanosynthesis. Given the properties of biofluids described above, bioleaching and biotransformation clearly offer a viable top–down route to near room temperature nanosynthesis of such complex systems.

Glass is a complex functional material that is found in diversified applications ranging from window panes, optical gadgets, watches, contact lenses and goggles, bioactive glasses for tissue engineering, energy systems, chemical containers and microfluidic channels [8–10]. It is therefore of great interest to synthesize nanoparticles of glass for potential use as filler or additive materials in composites, paints etc. or for biomedical applications. Glasses are of various types with varying chemical compositions and microstructural properties. It is of interest then to examine whether and to what degree a top–down nanosynthesis approach can transfer the composition and constitution from the bulk glass to the synthesized nanoparticles. In this work we have used borosilicate glass for bio-processing and have shown that the nanoparticles thus synthesized have a glassy state along with the desired inclusion of boron. Borosilicate glass is a heat resistant glass with a very low thermal expansion coefficient (third of normal glass) and a low refractive index across the visible range. The corresponding nanoparticles may also find interesting applications exploiting these unique properties. Finally, we have also examined the bio-processed glass surface for any modifications.

Since the present work concerns fungal processing of glass a few remarks may be made about the available background knowledge related to bio-processing especially in the context of

* Corresponding authors.
E-mail addresses: a.ahmad@ncl.res.in (A. Ahmad), sb.ogale@ncl.res.in (S. Ogale).

0022-3093/$ - see front matter © 2008 Elsevier B.V. All rights reserved.
doi:10.1016/j.jnoncrysol.2008.03.025

bioleaching [1,3,5,6]. Although bioleaching is accomplished by several micro-organisms, its effectiveness varies for different organisms and ambient conditions. Bacteria and fungi have attracted particular attention in this regard. Several mechanisms such as acidolysis, complexolysis, redoxolysis and bioaccumulation are suggested to be involved in bioleaching. Compared to bacterial leaching, fungal leaching has the advantages of the ability to grow under higher pH, thereby being more suitable in bioleaching of alkaline solids, and rendering a relatively faster leaching. Acidolysis is shown to be the principal mechanism in bioleaching with *Aspergillus niger* [1,11]. The fungus has been reported to produce organic acids, which include citric, oxalic, and gluconic acids during bioleaching. In bioleaching of sand a two step process involving leaching of silica in the form of silicic acid followed by hydrolysis of silicate complexes has been suggested [12]. In other studies, the mechanism of fungal bioleaching is suggested to be complex and not simply a direct chemical attack on the minerals. Indeed, the micro-organism is suggested to participate in the process actively [4]. For example, as bioleaching proceeds and the chemical constitution of the ambient evolves, live bio-organism can dynamically change the battery of chemical it can secrete. This has been suggested to be the case for bioleaching of minerals using *Aspergillus* sp. and *Penicillium* sp. [4].

2. Experimental

For the extracellular bioleaching of glass cover slips a novel alkalotolerant and thermophilic fungus, *Humicola* sp., was isolated from self-heating compost from the Pune district of Maharashtra, India. It was maintained on MGYP (malt extract, glucose, yeast extract, and peptone) agar slants. Stock cultures were maintained by sub culturing at monthly intervals. After growing the fungus at pH 9 and 50 °C for 4 days, the slants were preserved at the temperature of 15 °C. From an actively growing stock culture, subcultures were made on fresh slants and after 4 days incubation at pH 9 and 50 °C, the same were used as the starting material for fermentation experiments. For the bioleaching of glass slides, the fungus was grown in 250 mL Erlenmeyer flasks containing 50 mL of MGYP medium which is composed of malt extract (0.3%), glucose (1%), yeast extract (0.3%), and peptone (0.5%). Sterile 10% sodium carbonate was used to adjust the pH of the medium to 9. After the pH of the medium was adjusted, the culture was grown with continuous shaking on a rotary shaker (200 rpm) at 50 °C for 96 h. After 96 h of fermentation, mycelia were separated from the culture broth by centrifugation (5000 rpm) at 20 °C for 20 min and then the mycelia were washed thrice with sterile distilled water under sterile conditions. The harvested mycelial mass (20 g of wet mycelia) was then resuspended in 100 mL of distilled water in 250 mL Erlenmeyer flasks at pH 9. Several glass slides (commercially available borosilicate cover slips) were then added to the solution and the same was put into a shaker at 50 °C (200 rpm) and maintained in the dark.

The various fractions of the bioleached solution (used for the treatment of the glass cover slips) were collected during the course of reaction, by separating the fungal mycelia from the aqueous component by filtration. The diluted bioleached solution was drop cast on a carbon coated copper grid and analyzed using Transmission Electron Microscope JEOL model 1200 EX instrument operated at an accelerating voltage of 120 kV at room temperature. HR TEM images were also obtained using FEI Technai G^2 system. FTIR spectra of all samples were recorded on Perkin Elmer spectrum one B in diffuse reflectance (DRS) mode. The AFM images were also recorded using Veeco multimode SPM Model-Nanoscope-IV to reveal and estimate the surface roughness changes due to fungal processing. X-ray diffraction data were recorded on Panalytical 'X' Pert PRO system, while X-ray photoelectron spectra were recorded on VG MicroTech ESCA 3000 instrument at a pressure $<1 \times 10^{-9}$ Torr.

3. Results and discussion

First, we analyzed the extracted solution for its contents. The corresponding transmission electron micrographs (Fig. 1 and the insets) bring out the formation of very tiny ($\sim 5 \pm 0.5$ nm) nearly monodispersed nanoparticles by the bioleaching process. The histogram shown in the top inset clearly brings out the extremely narrow nanoparticle size distribution. As stated earlier, in addition to organic acids the biofluids also have a set of proteins, which play a role of capping agents in the process. As the dissolved components get into the solution, they form reactive molecular complexes (that eventually lead to the inorganic nanoparticles) that are also dynamically capped by the proteins present. This arrests the growth of the complexes and hence that of the corresponding nanoparticles thus formed. Preliminary gel electrophoresis measurements indicate that the fungus secretion exhibits four distinct protein related bands, distinct with respect to their electro-mobility; the latter being a collective function of their molecular weights, mobility and other characteristics. One or more of such proteins may be the enzymes that act as the leaching agents as well as the capping agents for the extracted silicate nanoparticles (NPs). The presence of high concentration of such functionalizable proteins should explain the tiny size of the nanoparticles.

In order to confirm the constitution of the nanoparticles, X-ray diffraction, FTIR and X-ray photoelectron spectroscopy (XPS) techniques were employed. The X-ray diffraction data shown in Fig. 2 compare the patterns for the parent glass (a), the as-extracted nanoparticles (b), and the nanoparticles sintered at 500 °C (c). The characteristics of the parent glass and those of as-extracted nanoparticles compare favourably, although there are small differences in details, which can be attributed to structural relaxations that can be expected in ultrafine nanoparticles [13]. In particular, the primary lattice reflection is more weighted towards smaller 2θ or larger d-value. For the annealed NP sample a host of well-defined peak structures are seen to develop. These can be appropriately marked by various peaks corresponding to silica, silicate

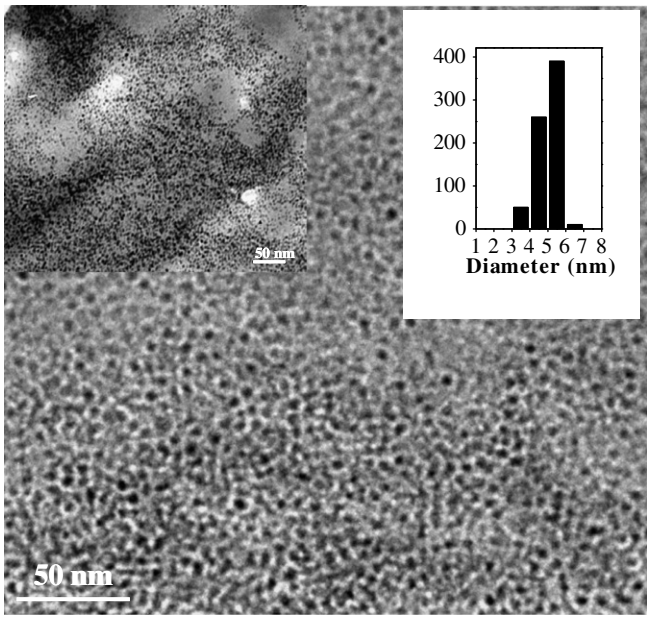

Fig. 1. Transmission electron micrographs of the nanoparticles obtained by bioleaching of glass and biotransformation.

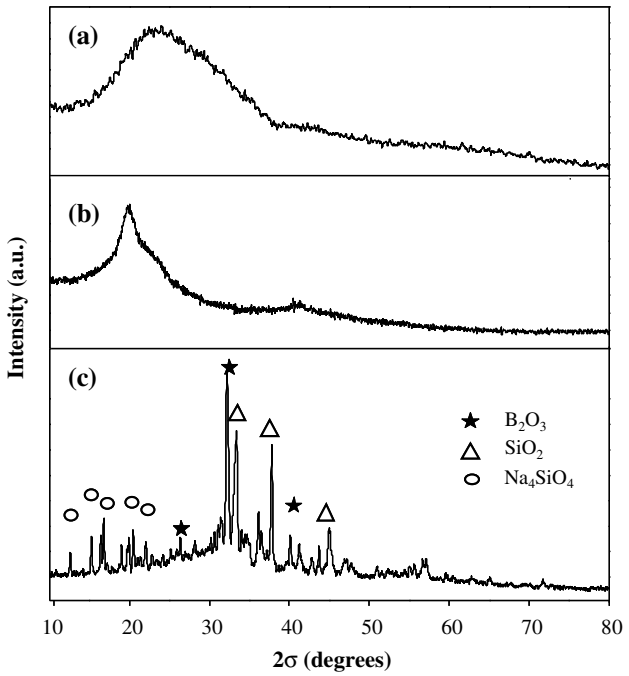

Fig. 2. Comparison of X-ray diffraction patterns of (a) parent glass, (b) as-extracted nanoparticles and (c) nanoparticles sintered at 500 °C.

and boron oxide phases (JCPDS card PDF # 43-1300, 27-0784, 44-1085). This shows that the as-extracted nanoparticles do represent an amorphous glassy network phase comprising of various elements such as Si, Na, B, O resembling the parent glass and the same get decomposed upon annealing at high temperature. It is very interesting that most elements in the parent compound are extracted into the synthesized nanoparticles by the bioleaching process. This shows that the presence of multiple complex etchants in a biofluid have a collective ability to activate nearly stoichiometric extraction and biotransformation.

FTIR measurements were done to identify the specific bonding configurations in the samples. The specific interest was to examine whether boron related bonds are present in the NPs which could qualify it as a borosilicate rather than just silica (SiO_2) NPs. Thus, in Fig. 3(A) we compare the FTIR spectra for the cases of as-extracted (a) and 500 °C annealed (b) NPs. We also present in the same figure the FTIR data for pure silica (SiO_2) NPs (c) synthesized in our laboratory by chemical method, and commercial B_2O_3 (d) for comparison. The various stretching and bending modes identified in the published literature have also been indicated [14–17]. These data suggest presence of the signatures of ν Si–O–Si, δ B–O–Si, ν B–O–Si, ν B–O bonds. This implies that the extracted nanoparticles are borosilicate type. The presence of boron in the extracted nanoparticles was further confirmed by XPS. The corresponding data for the parent glass (a) and the drop cast film of extracted NPs (b) on the zirconia substrate are shown in Fig. 3(B). The signatures at 190.68 eV and 191.32 eV in the two cases correspond to boron (B 1s), albeit shifted due to small differences in the nature of bonding between the bulk and the nanoparticles [18,19]. Upon annealing, the peaks are seen to evolve and shift as expected and indicated by the four arrows. For instance the signature indicated by "4" (which is better defined than that in curve "a") is close to but shifted with reference to the corresponding sharper signature in curve c for pure silica particles. Similarly signature "1" is close to that in B_2O_3 and "3" overlaps well with those in curves c and d for pure silica and B_2O_3. This is consistent with the evolution suggested by XRD upon annealing wherein phases of SiO_2, B_2O_3 are seen to form.

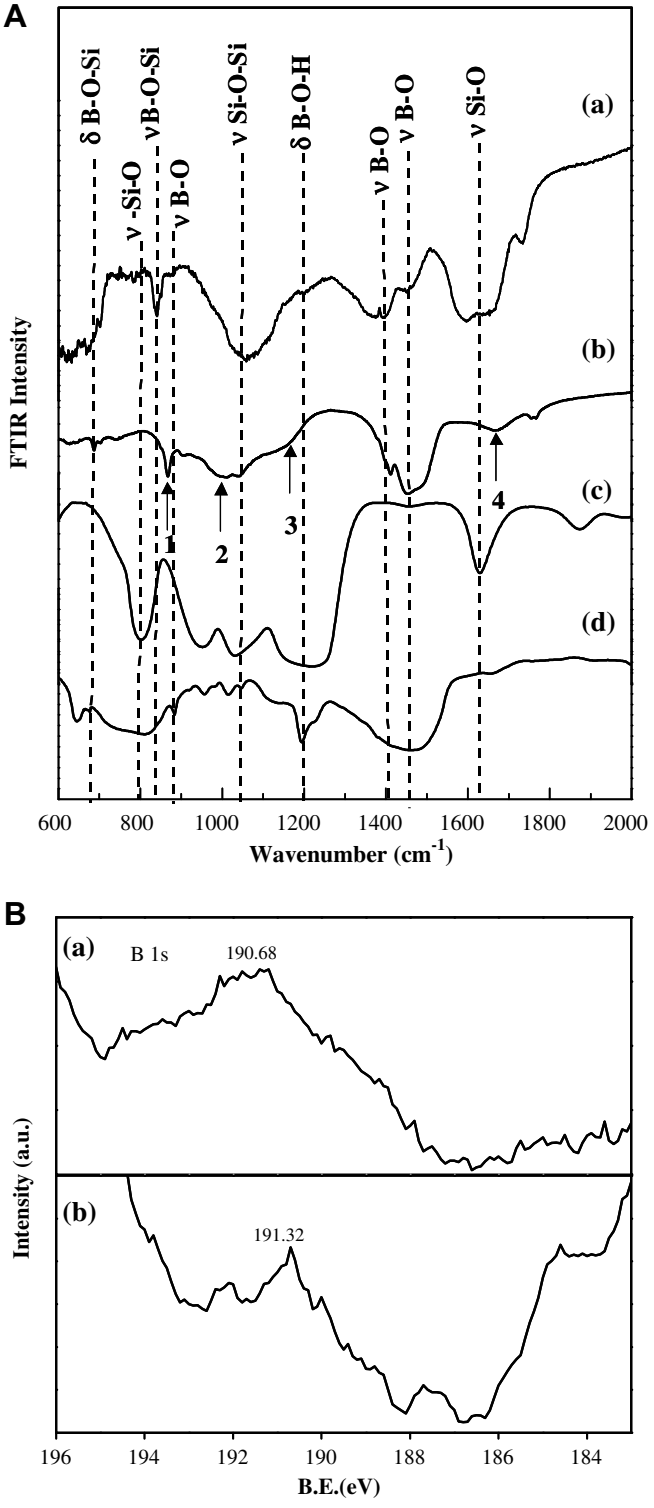

Fig. 3. (A) Comparsion of FTIR data for (a) as-extracted silicate nanoparticles, (b) nanoparticles after annealing at 500 °C, (c) silica (SiO_2) nanoparticles (100 nm) prepared by stober's method, and (d) commercial B_2O_3 powder; (B) X-ray photoelectron spectroscopy data for boron (B 1s) for (a) parent glass and (b) drop cast film of extracted nanoparticles on zirconia substrate.

In Fig. 4 we present the state of other elements seen in the XPS spectra of the parent glass, the extracted nanoparticles (drop cast film) and the bioleached glass surface. In the parent glass (a) case, characteristic Si 2p and O 1s peaks are observed at binding energy values of 103.2 eV and 532.64 eV, respectively, as expected. Interestingly, in the case of the drop cast NPs film (b) and the fungal

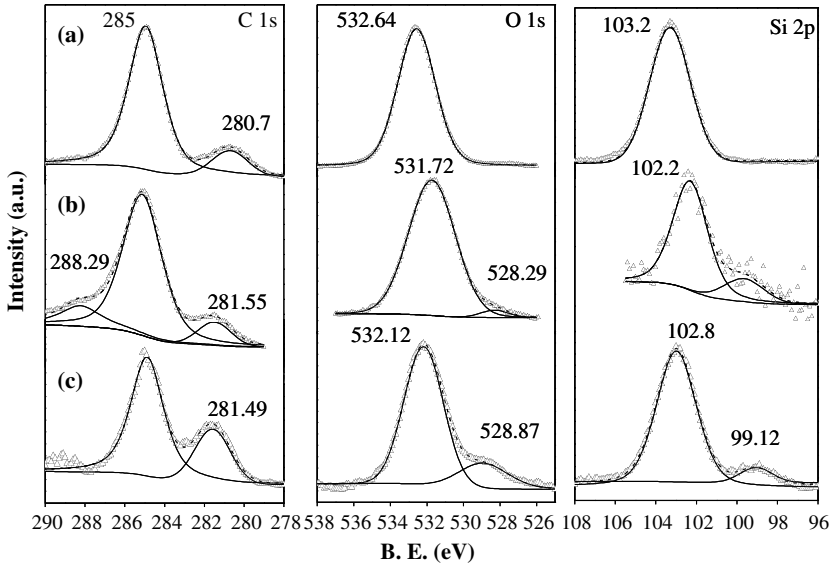

Fig. 4. X-ray photoelectron spectroscopy data for (a) parent glass, (b) the drop cast film of as-extracted nanoparticles on zirconia substrate, and (c) bioleached glass respectively; the triangles represent the experimental data and the solid lines represent the fits to the data.

processed glass surface (c) additional peaks appear on the lower binding energy side for both Si 2p and O 1s at 99.12 eV and 528.87 eV, respectively. Moreover, shifts in the main peak positions towards lower energy are also observed, the shifts being slightly higher for the nanoparticles as expected due to relaxations. We also observed increase in the C 1s contribution towards its low energy side. But since it appears in the same region as that for adventitious carbon resulting from system hydrocarbon, it can simply be due to the enhanced adsorption area due to roughness as well as due to the extra proteins.

Significant, compositionally dependent changes are known to occur in the O 1s spectra of glass samples. Previous studies have

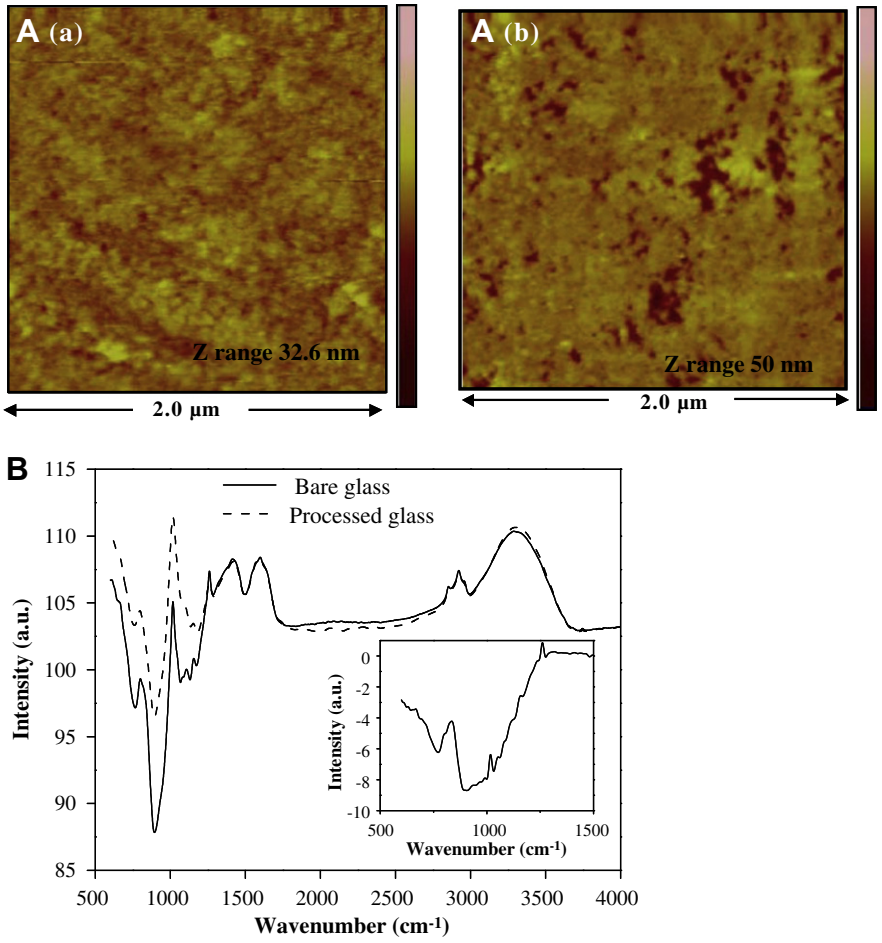

Fig. 5. (A) Atomic Force micrographs (AFM) and (B) FTIR spectra, respectively, for (a) the parent glass and (b) fungal processed (15 h) glass cover slips.

established that the larger binding energy peak (~532 eV) in the spectrum is due to bridging oxygen (BO) which is covalently bound to two silicon atoms (Si–O–Si), and the smaller binding energy peak (~529 eV) is due to non-bridging oxygen (NBO) which is covalently bound to one silicon and ionically bound to an alkali ion such as sodium (Si–O–Na) [20–23]. Indeed, the intensities of the photoelectrons from these oxygen types bonded in different ways and the corresponding relative chemical shifts could be correlated with alkali and alkaline earth oxide contents and with the related cation field strengths. Moreover, the ionic binding character introduced into the glass networks by the alkali and alkaline earth ions is a non-localized effect because not only the NBO atoms are influenced but the BOs as well [25]. With increasing alkali element fraction the line positions are shifted to lower binding energy [26]. The intensity ratio of NBO/BO and their energy separation depend on the content of the silica network modifier introducing NBO. The XPS and FTIR data thus together imply that chemical modification, especially the enhancements of NBO accompanies the bioleaching process and is present in the NPs as well as the processed glass surface.

Fig. 5(A) compares the atomic force micrographs (AFM) for the parent (A(a)) and fungal processed (15 h) glass cover slips (A(b)). The root mean square roughness was seen to increase from 1.27 nm for bare glass to 2.52 nm for 15 h processed case. It has been reported that RMS roughness of this order is generated on the glass surface by high temperature annealing at temperatures above 500 °C [24]. It is very interesting that the same is generated by fungal processing at 50 °C. We also compared the FTIR spectra for the same two cases of interest (Fig. 5(B)). When normalized at long wavelength, the spectra show significant changes in the 500–1200 cm^{-1} region, and small differences in the neighbourhood of 1800–2600 cm^{-1}. The spectral features in low frequency region are known to result from the Si–O–Si network (stretching mode in the range 1000–1300 cm^{-1}, Si–O–Si bending vibrations around 800 cm^{-1} etc.) [20,25,26]. Thus, the network is clearly influenced by fungal processing and represents an important aspect of chemical modification. We believe that the mild and controlled surface modification of glass by fungal processing may have applications in different fields.

4. Conclusion

In conclusion, we have demonstrated the use of fungus based bioleaching for the synthesis of water dispersible nearly monodispersed ultrafine (~5 ± 0.5 nm) silicate nanoparticles coated with a natural secreted protein and have shown that the processed glass surface also undergoes significant morpho-chemical modification. Various characterizations are used to demonstrate that fairly stoichiometric extraction and nanosynthesis are possible by bioleaching and biotransformation.

Acknowledgments

One of us (SBO) would like to thank the Department of Science and Technology (DST), Govt. of India for the award of Ramanujan Fellowship. Authors acknowledge DST for setting up a unit on Nanoscience and Technology (DST-UNANST) at NCL, Pune, India. AA would like to thank the Department of Biotechnology (DBT), Govt. of India for Tata Innovation fellowship award.

References

[1] C.N. Mulligan, M. Kamali, J. Chem. Technol. Biotechnol. 78 (2003) 497.
[2] D.E. Rawlings, J. Ind. Microbiol. Biotechnol. 20 (1998) 26874.
[3] Hung-Yee Wu, Yen-Peng Ting, Enzyme Microbial Technol. 38 (2006) 839.
[4] M. Valix, F. Usai, R. Malik, Minerals Eng. 14 (2001) 197.
[5] H.L. Ehrlich, Chem. Geol. 132 (1996) 5.
[6] I. Styriakova, I. Styriak, M.P. Nandakumar, B. Mattiasson, J. Microbiol. Biotechnol. 19 (2003) 583.
[7] E.K. Moira, K. Henderson, R.B. Duff, J. Soil Sci. 14 (1963) 236.
[8] D.C. Boyd, J.F. MacDowell, Adv. Ceram. 18 (1986) 157.
[9] A. Duparré, M. Flemming, J. Steinert Reihs, K. Fraunhofer, IOF Annual Report, 38, 2001.
[10] I.D. Xynos, M.V.J. Hukkanen, J.J. Batten, L.D. Buttery, L.L. Hench, J.M. Polak, Calcified Tissue Int. 67 (2000) 321.
[11] N. Hall, A.B. Tomsett, Microbiology 146 (2000) 1399.
[12] V. Bansal, A. Sanyal, D. Rautaray, A. Ahmad, M. Sastry, Adv. Mater. 17 (2005) 889.
[13] J. Pérez-Pariente, F. Balas, M. Vallet-Regı, Chem. Mater. 12 (2000) 750.
[14] C. Canevali, R. Scotti, A. Vedda, M. Mattoni, F. Morazzoni, L. Armelao, D. Barreca, G. Bottaro, Chem. Mater. 16 (2004) 315.
[15] G.D. Soraru, N. Dallabona, C. Gervais, F. Babonneau, Chem. Mater. 11 (1999) 910.
[16] O.M. Moon, B.C. Kamg, S.-B. Lee, J.-H. Boo, Thin Solid Films 464 (2004) 64.
[17] Q. Yang, J. Sha, L. Wang, Yu. Zou, J. Niu, C. Cui, D. Yang, Physica E 27 (2005) 319.
[18] M.M. Ennaceur, B. Terreault, J. Nucl. Mater. 280 (2000) 33.
[19] M. Belyansky, M. Trenary, Surf. Sci. Spectra, 3 147 (1995).
[20] A. Mekki, D. Holland, C.F. MacConville, J. Non-Cryst. Solids 215 (1997) 271.
[21] Y. Miura, H. Kusano, T. Nanba, S. Matsumoto, J. Non-Cryst. Solids 290 (2001) 1.
[22] R. Brückner, H.-U. Chun, H. Goretzki, M. Sammet, J. Non-Cryst. Solids 42 (1980) 49.
[23] J. Zemek, P. Jiricek, O. Gedeon, B. Lesiak, A. Jozwik, J. Non-Cryst. Solids 351 (2005) 1665.
[24] H.K. Jang, S.W. Whangbo, Y.K. Choi, K. Jeong, C.N. Whang, C.H. Wang, D.J.S. Choi Lee, J. Non-Cryst. Solids 296 (2001) 182.
[25] J. Serra, P. Gonzalez, S. Liste, C. Serra, S. Chiussi, B. Leon, M. Perez- Amor, H.O.M. Ylanen Hupa, J. Non-Cryst. Solids 332 (2003) 20.
[26] A. Agarwal, M. Tomozawa, J. Non-Cryst. Solids 209 (1997) 166.